Jour. of the KGS Vol. 17, No. 3. June 2001, pp 83~94

# A Study on the Behavior of Multi-tiered Reinforced Earth Retaining Wall

# 다단식 보강토 옹벽의 거동특성 연구

Yoo, Han-Kyu*1 유 한 규
Han, Suk-Joon*2 한 석 준
Park, Eon-Sang*3 박 언 상

## 요 지

본 연구에서는 상・하단으로 구분된 2개의 동일한 보강토옹벽에 대해서 상호 이격거리에 따른 수치해석을 수행하여 전면벽체의 수평변위, 전면벽체 배면의 수평토압, 보강토체 배면의 수평토압 그리고 보강재의 최대인장력 분포 및 크기변화 양상등 다단식 보강토옹벽의 거동을 살펴보았다. 또한, 하단 옹벽에 증가되는 응력을 산정하고자 중첩의 원리를 적용한 2:1 응력분포법을 제시하였다. 수치해석 결과 이격거리가 증가함에 따라 상단옹벽이 하단옹벽에 미치는 영향이 감소하였으며 하단 옹벽 높이의 두 배이상 이격시, 상호 거동은 독립옹벽으로 거동하였다. 하단 옹벽내 응력 산정방법에 있어서 NCMA의 방법이 가장 보수적인 결과를 보였으며 본 연구에서 제시한 2:1 응력분포법중 주동파괴면을 고려하지 않은 방법이 수치해석 결과와 가장 유사하게 나타났다.

## Abstract

In this study, in order to assess the behaviour of multi-tiered reinforced earth retaining walls, two reinforced earth retaining walls which have the identical geometry and configuration are presented and analyzed in the cases of several set back distances. The horizontal displacement of facing, lateral earth pressure behind both facing and reinforced earth body, and maximum tensile forces in reinforcement are obtained from the numerical analysis. Also, 2:1 stress distribution method based on superposition principle is proposed to estimate the increasing stress distribution of the lower wall due to the upper wall. The results of analysis show that the influence of the upper wall on the lower one decreases according to the increase of set back distance, and when the set back distance is two times as great as the height of the lower one, the behaviour of each wall works independently. When the increasing stress of the lower wall due to the upper one was calculated, NCMA(National Concrete Masonry Association) method using uniform surcharge was the most conservative, and the stress increase obtained from 2:1 method without consideration of active failure surface was similar to the result of numerical analysis.

**Keywords** : Multi-tiered, Reinforced earth retaining wall, 2:1 method, Superposition, Set back distance

## 1. Introduction

Reinforced earth retaining walls have been recently substituted for conventional concrete retaining walls because of their merits in construction, economy, and seismic performance. Since most of the areas have no

*1 Member, Assistant Professor, Dept. of Civil and Environmental Engrg., Hanyang Univ.
*2 Member, M.S Student, Dept. of Civil and Environmental Engrg., Hanyang Univ.
*3 Member, Ph.D Candidate, Dept. of Civil and Environmental Engrg., Hanyang Univ.

sufficient construction site, the construction of high retaining walls can gradually increase. In this case, multi-tiered lower wall can be constructed instead of such a high wall owing to construction, economy, and stability (Jalla, 1999). In single reinforced earth retaining walls, the analysis or the design method is well established (KGS, 1998). When the multi-tiered reinforced earth retaining wall is designed, however, the load of upper wall is regarded simply as uniform surcharge(NCMA, 1997). Recently there were few studies on the behaviour of such walls, but these studies were done according to just one or two set back distances(Yoo, 2000). But the location of failure surface as well as the mutual behaviour of upper and lower wall according to set back distance is not well established. Specially in the case of more than two walls, the behaviour will be more complicated than single wall, so that the mutual behaviour of multi-tiered reinforced earth retaining wall must be analyzed and studied for the establishment of design methods.

In this study, in oder to assess the behaviour of such multi-tiered walls, two reinforced earth retaining walls which have the identical geometry and configuration are presented and analyzed. The horizontal displacement of facings, horizontal earth pressure behind both facing and reinforced earth body, and maximum tensile forces in the reinforcements are obtained from numerical analysis in cases of several set back distances. The NCMA method and 2:1 stress distribution method based on the superposition principle are used to estimate the increasing stress distribution of the lower wall due to the upper wall. The critical set back distance in which the upper and the lower wall can be treated as each independent wall is checked as well.

## 2. Method of Estimating Stress Increase

### 2.1 NCMA Method

In the multi-tiered earth retaining wall, the upper reinforced retaining wall plays a role of dead load for the lower reinforced retaining wall. If surcharge is located inside the lateral distance less than two times of the distance of the lower reinforced earth retaining wall height, the surcharge will be loaded at the lower reinforced earth retaining wall. Fig. 1 can be used to calculate equivalent distribution load applied from the upper to the lower in internal and external stability analysis of multi tiered earth retaining walls. The approximate surcharge to the lower reinforced earth retaining wall is presented in Table 1.

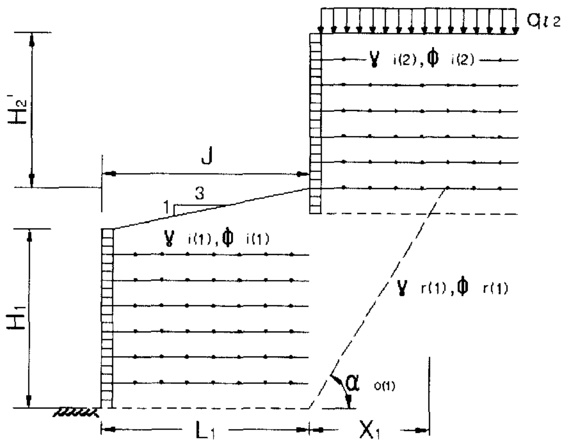


J = Lateral set back distance between the upper and the lower wall
$L_1$ = Length of reinforcement + width of block
$X_1$ = $(H_1+J/S)\tan\alpha_{o(1)}$
S = 500 for horizontal backfill between walls where, $H_1>H_2'$

Fig. 1 Description of multi-tiered reinforced earth retaining wall (NCMA, 1997)

### 2.2 2:1 Method

To check the external and internal stability of reinforced retaining wall according to the set back distance between upper and lower wall, the estimation of the stress increment in the lower wall due to the upper wall is required. Therefore the 2:1 method based on superposition principle is proposed to estimate such stress increment. The proposed method is derived for the case with considering active failure surface as well as the case without considering active failure surface.

#### 2.2.1 External Stability

In checking the external stability of the lower wall

Table 1. Surcharge application (NCMA, 1997)

| Internal Stability | | External Stability | |
|---|---|---|---|
| $J > L_1$ | No Effect<br>$q_{d1} = 0$<br>$q_{l1} = 0$ | $J > (L_1 + X_1)$ | No Effect<br>$q_{d1} = 0$<br>$q_{l1} = 0$ |
| $0.3L_1 < J < L_1$ | Partial Surcharge Application<br>$q_{d1} = \frac{(L_1 - J)}{L_1}(\gamma_{i(2)} H_2')$<br>$q_{l1} = \frac{(L_1 - J)}{L_1}(q_{l2})$ | $(L_1 + 0.5X_1) < J < (L_1 + X_1)$ | Partial Surcharge Application<br>$q_{d1} = \frac{(L_1 + X_1 - J)}{X_1}(\gamma_{i(2)} H_2')$<br>$q_{l1} = \frac{(L_1 + X_1 - J)}{X_1}(q_{l2})$ |
| $J < 0.3L_1$ | Total Surcharge Application<br>$q_{d1} = \gamma_{i(2)} H_2'$<br>$q_{l1} = q_{l2}$ | $J < (L_1 + 0.5X_1)$ | Total Surcharge Application<br>$q_{d1} = \gamma_{i(2)} H_2'$<br>$q_{l1} = q_{l2}$ |

* $q_{d1}$ $q_{l1}$ : the self-weight and live load of the upper reinforced earth retaining wall, respectively

considering the active failure surface, four different locations of upper wall must be considered as shown in Fig. 2 and Table 2. In this figure and table, $q$ is the uniform surcharge due to the self-weight of the upper wall and $q_m$ is the Meyerhof's pressure distribution considering the effects of the backfill thrust in the upper wall, and then $q'$ is the strip load which is deducted $q$ from $q_m$ . That is to say, $q' = q_m - q$.

Among the four different cases, the case 3 is considered and analyzed in this section. Fig. 3 shows the case that both $q$ and $q'$ exist partially in active failure

Table 2. Locations of the upper wall in external stability

| Load / Case | q | q' |
|---|---|---|
| 1 | Zone A ~ ∞ | Zone A ~ B |
| 2 | Zone A ~ ∞ | Zone A ~ C |
| 3 | Zone B ~ ∞ | Zone B ~ C |
| 4 | Zone C ~ ∞ | Zone C |

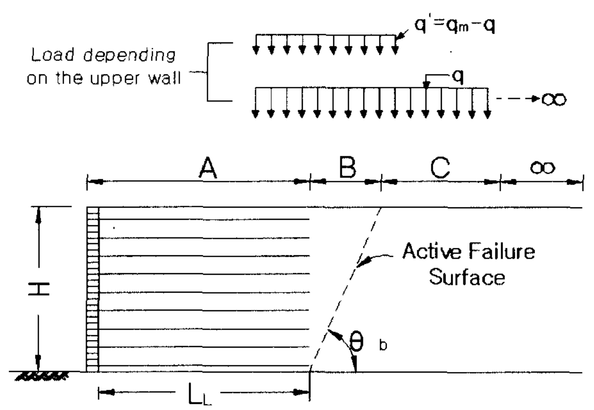


Fig. 2 Zones of the upper wall in external stability

area $X_b$ behind the lower reinforced body.

$\Delta\sigma_{v(q)}$ is equal increment in all depth by infinite uniform distributed load. $\Delta\sigma_{v(im)}$ is the increment of vertical stress due to the imaginative strip load. Because strip load $q$ with width of $D - L_1$ is supplementary in calculating $\Delta\sigma_{v(q)}$, increment by the supplementary $q$ needs to be deducted from $\Delta\sigma_{v(q)}$. $\Delta\sigma_{v(q')}$ is increment of vertical stress by load $q'$ with width of $b_f$ existing in active failure area $X_b$ behind the reinforced earth body. In the process, using superposition principle, the sum of increment of vertical stress behind reinforced body can be expressed as follows:

$$\Delta\sigma_v = \Delta\sigma_{v(q)} - \Delta\sigma_{v(im)} + \Delta\sigma_{v(q')} \tag{1}$$

Fig. 4 shows 2:1 stress distribution method to calculate $\Delta\sigma_{v(im)}$ by imaginative strip load and it can be calculated by Eq. (2).

$$\Delta\sigma_{v(im)} = \frac{b_f \times q}{d} \tag{2}$$

Where

$$b_f = D - L_1$$

$$d = b_f + \frac{z}{2}$$

Fig. 5 shows 2:1 stress distribution method to calculate $\Delta\sigma_{v(q')}$. According to the depth influencing on horizontal earth pressure behind the lower reinforced earth body, $\Delta\sigma_{v(q')}$ is calculated by Eq. (3) and Eq. (4).

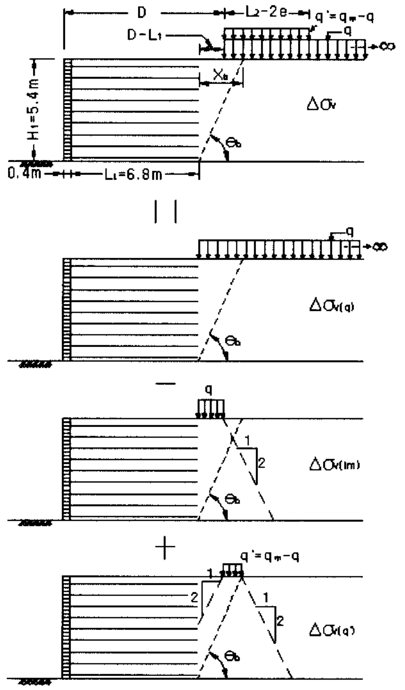


Fig. 3 Superposition application in the analysis of external stability considering active failure surface

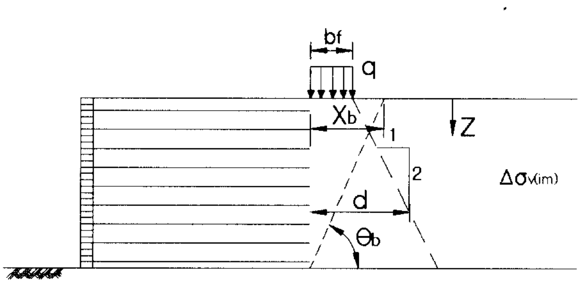


Fig. 4 2:1 stress distribution method(external stability) in calculating $\Delta\sigma_{v(im)}$ considering active failure surface

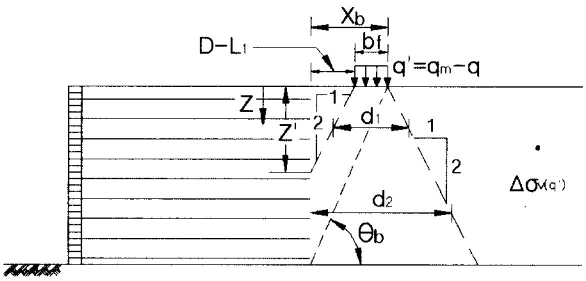


Fig. 5 2:1 stress distribution method(external stability) calculating $\Delta\sigma_{v(q')}$ considering active failure surface

When $z \leq z'$,

$$d_1 = b_f + z$$

$$\Delta\sigma_{v(q')} = \frac{b_f \times q'}{d_1}$$

$$\Delta\sigma_{h(q')} = 0 \tag{3}$$

When $z > z'$,

$$d_2 = b_f + \frac{z}{2} + D - L_1$$

$$\Delta\sigma_{v(q')} = \frac{b_f \times q'}{d_2}$$

$$\Delta\sigma_{h(q')} \neq 0 \tag{4}$$

Where $b_f = X_b - (D - L_1)$

$z' = 2 \times (D - L_1)$

In checking the external stability of the lower wall without considering the active failure surface, the similar procedure can be used. In this procedure, full width of surcharge area has to be used to calculate the stress increment using 2:1 method.

### 2.2.2 Internal Stability

In checking the internal stability of the lower wall considering the active failure surface, three different locations of upper wall must be considered as shown in Fig. 6 and Table 3.

Table 3. Locations of the upper wall in internal stability

| Load / Case | q | q' |
|---|---|---|
| 1 | Zone A ~ ∞ | Zone A ~ B |
| 2 | Zone B ~ ∞ | Zone B or B ~ C |
| 3 | Zone C ~ ∞ | Zone C |

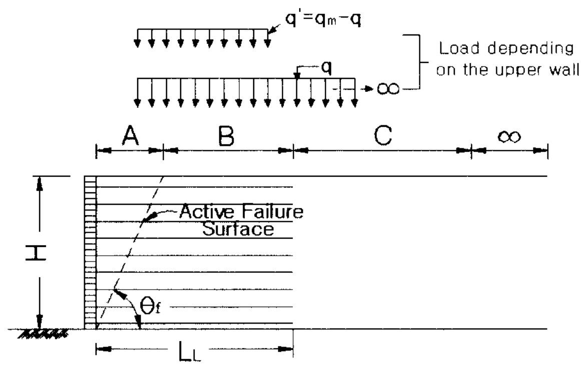


Fig. 6 Zones of the upper wall in internal stability

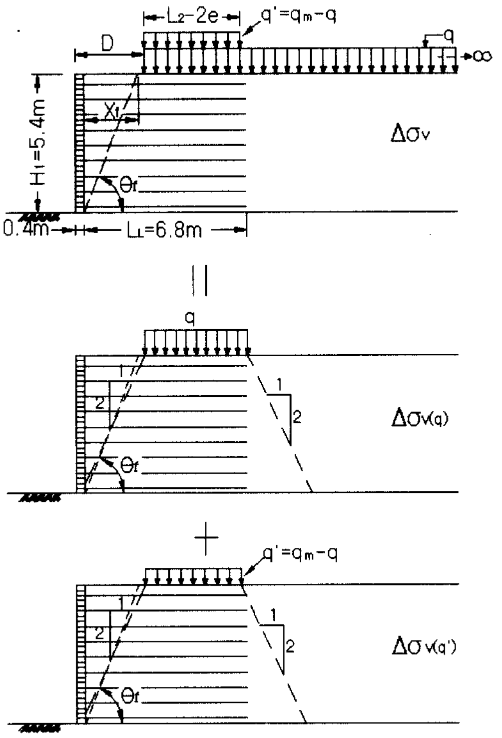


Fig. 7 Superposition application in analysis of internal stability considering active failure surface

Among the three different cases, case 2 is considered and analyzed in this section. Fig. 7 shows the case that both $q'$ and $q$ exist outside the active failure surface $X_f$ behind the facing of the lower wall. The increment of vertical stress for the strip load, $q'$ and $q$ according to depth can be calculated by 2:1 stress distribution method. In the process, using superposition principle, the sum of increment of vertical stress behind the facing of the lower wall can be expressed as follows:

$$\Delta\sigma_v = \Delta\sigma_{v(q)} + \Delta\sigma_{v(q')} \tag{5}$$

Fig. 8 shows 2:1 stress distribution method and $\Delta\sigma_{v(q)}$ can be calculated by Eq. (6) and Eq. (7).

When $z \le z'$,

$$d_1 = b_f + z$$

$$\Delta\sigma_{v(q)} = \frac{b_f \times q}{d_1}$$

$$\Delta\sigma_{h(q)} = 0 \tag{6}$$

When $z > z'$,

$$d_2 = b_f + \frac{z}{2} + D'$$

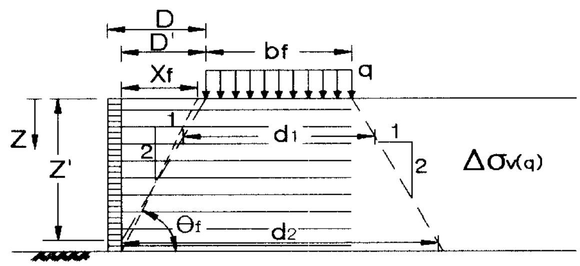


Fig. 8 2:1 stress distribution method(internal stability) in calculating $\Delta\sigma_{v(q)}$ considering active failure surface

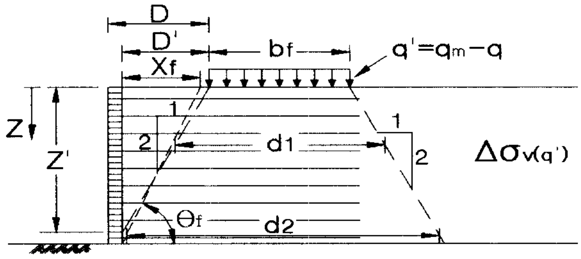


Fig. 9 2:1 stress distribution method (internal stability) in calculating $\Delta\sigma_{v(q)}$ considering active failure surface

$$\Delta\sigma_{v(q)} = \frac{b_f \times q}{d_2}$$

$$\Delta\sigma_{h(q)} \neq 0 \tag{7}$$

Where $b_f = L_1 - D$

$L_1 = block\ width + L_L$

$z' = 2 \times D'$

Fig. 9 shows 2:1 stress distribution method to calculate $\Delta\sigma_{v(q')}$. The width $b_f$ of $q'$ can be inside or outside the lower reinforced earth body. The former considers the width of $L_2 - 2e$ and the latter only considers the width of $L_1 - D$. The increment of vertical stress can be calculated by Eq. (3) and Eq. (4) according to depth affecting the facings. But $d_1$, $d_2$, and $b_f$ in Eq. (3) and Eq. (4) are as follows.

When $z \le z'$ When $z > z'$

$d_1 = b_f + z$ $d_2 = b_f + \frac{z}{2} + D'$

$\Delta\sigma_{h(q')} = 0$ $\Delta\sigma_{h(q')} \neq 0$

Where $z' = 2 \times D'$

$b_f = L_2 - 2e$ for $L_2 - 2e \le L_1 - D$

$b_f = L_1 - D$ for $L_2 - 2e > L_1 - D$

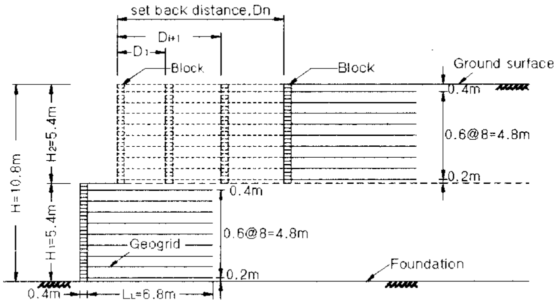


Fig. 10 Schematic view of multi-tired reinforced earth retaining wall

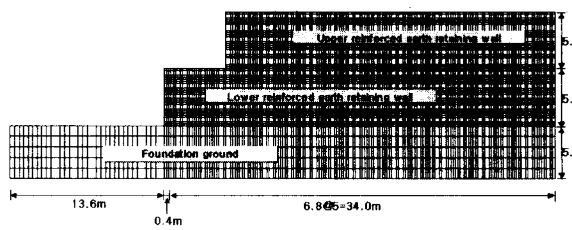


Fig. 11 Finite difference grid used in the analysis

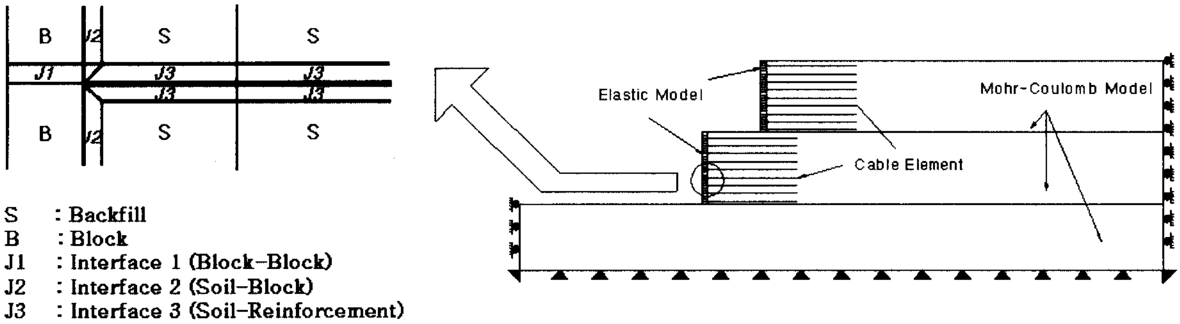


Fig. 12 Constitutive model and boundary condition

In checking the internal stability of the lower wall without considering the active failure surface, the similar procedure can be used. In this procedure, full width of surcharge area has to be used to calculate the stress increment using 2:1 method.

## 3. Numerical Analysis

In this study, two earth retaining walls reinforced by geogrids which have the identical geometry and configuration are considered. The height of each wall is 5.4m and the length of reinforcement is 6.8m as shown in Fig. 10. A total of 16 set back distances measured from the facing of the lower wall are used to investigate their effects on the behavior of multi-tired reinforced earth retaining wall.

For the numerical analysis, the FLAC$^{2D}$ program based on finite difference method is used. The properties of soil and reinforcement used in FLAC$^{2D}$ program are summarized in Table 4 and the finite difference grid used in the analysis is shown in Fig. 11.

The block of the upper and the lower reinforced retaining wall is assumed to be elastic material, and the foundation as well as the backfill soils is simulated by Mohr-Coulomb model. Also, the reinforcements are modeled as cable elements. Fig. 12 shows the constitutive model and boundary condition. In this model, the inter-

Table 4. Properties of soil and reinforcement used in the analysis

| Section | elastic modulus E (Pa) | density ρ (kg/m$^3$) | cohesion C (Pa) | friction ϕ (deg) | Poisson's ratio ν | area A (m$^2$) | yielding strength (N) |
|---|---|---|---|---|---|---|---|
| backfill | 5.00×E7 | 1800 | 0 | 35 | 0.3 | N/A | N/A |
| retained soil | 5.00×E7 | 1800 | 0 | 35 | 0.3 | N/A | N/A |
| foundation | 5.00×E7 | 1900 | 0 | 40 | 0.3 | N/A | N/A |
| block | 5.00×E9 | 2300 | 0 | N/A | 0.3 | N/A | N/A |
| reinforements | 2.00×E9 | 10.2 | 0 | N/A | N/A | 4.92×E-4 | 1.129×E5 |

Table 5. Values of input parameters used in the interface element

| section | vertical stiffness Kn (Pa/m) | shear stiffness Ks (Pa/m) | friction angle φ (deg) | bond stiffness of cable $K_b$ (N/m/m) | bond strength of cable $S_b$ (N/m) |
|---|---|---|---|---|---|
| interface 1 (block/block) | 9.80×E8 | 9.80×E7 | 35 | N/A | N/A |
| interface 2 (block/backfill) | 9.80×E8 | 9.80×E5 | 23.33 | N/A | N/A |
| interface 3 (reinforements/backfill) | N/A | N/A | N/A | $480 \cdot \gamma \cdot z$ | $1.12 \cdot \gamma \cdot z$ |

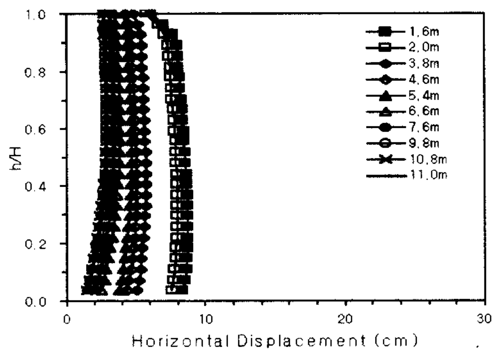


Fig. 13 Horizontal displacement in the facing of the upper wall

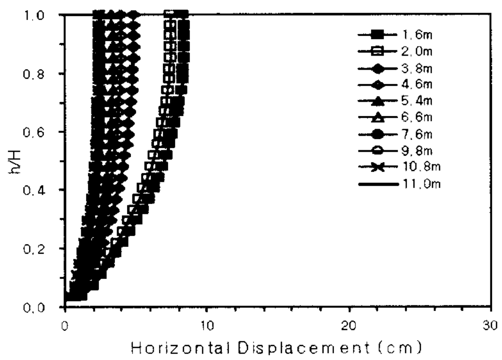


Fig. 14 Horizontal displacement in the facing of the lower wall

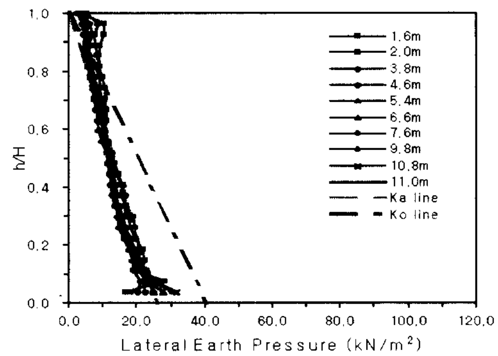


Fig. 15 Lateral earth pressure behind the facing of the upper wall

face elements are used to allow the slip along the interface between block and block, block and backfill as well as reinforcements and backfill. The values of input parameters used in interface elements are summarized in Table 5.

From the numerical analysis, the horizontal displacement of facing, lateral earth pressure behind both facing and reinforced earth body, and maximum tensile forces in the reinforcements are obtained, and the results of the analysis are presented in the following sections.

## 4. Discussion of Results

### 4.1 Horizontal Displacement of Facing

Figs. 13 and 14 present the relationship between nondimensional height $h/H$ and horizontal displacement of facing. In the figures, $h$ is the height of location measured from the bottom of each wall and $H$ is the height of each wall.

As shown in Figs. 13 and 14, the horizontal displacement of facing of both upper and lower walls tends to decrease with increasing set back distance. In the case of upper wall, the decrease in horizontal displacement may be attributed to the decrease of relaxation area of lower reinforced earth body. In the case of lower wall, as the set back distance increases, the effects of load of upper wall on the facing of lower wall decrease and then the horizontal displacement decreases. The displacement of both the upper and lower walls becomes constant when the set back distance is greater than 10.8m.

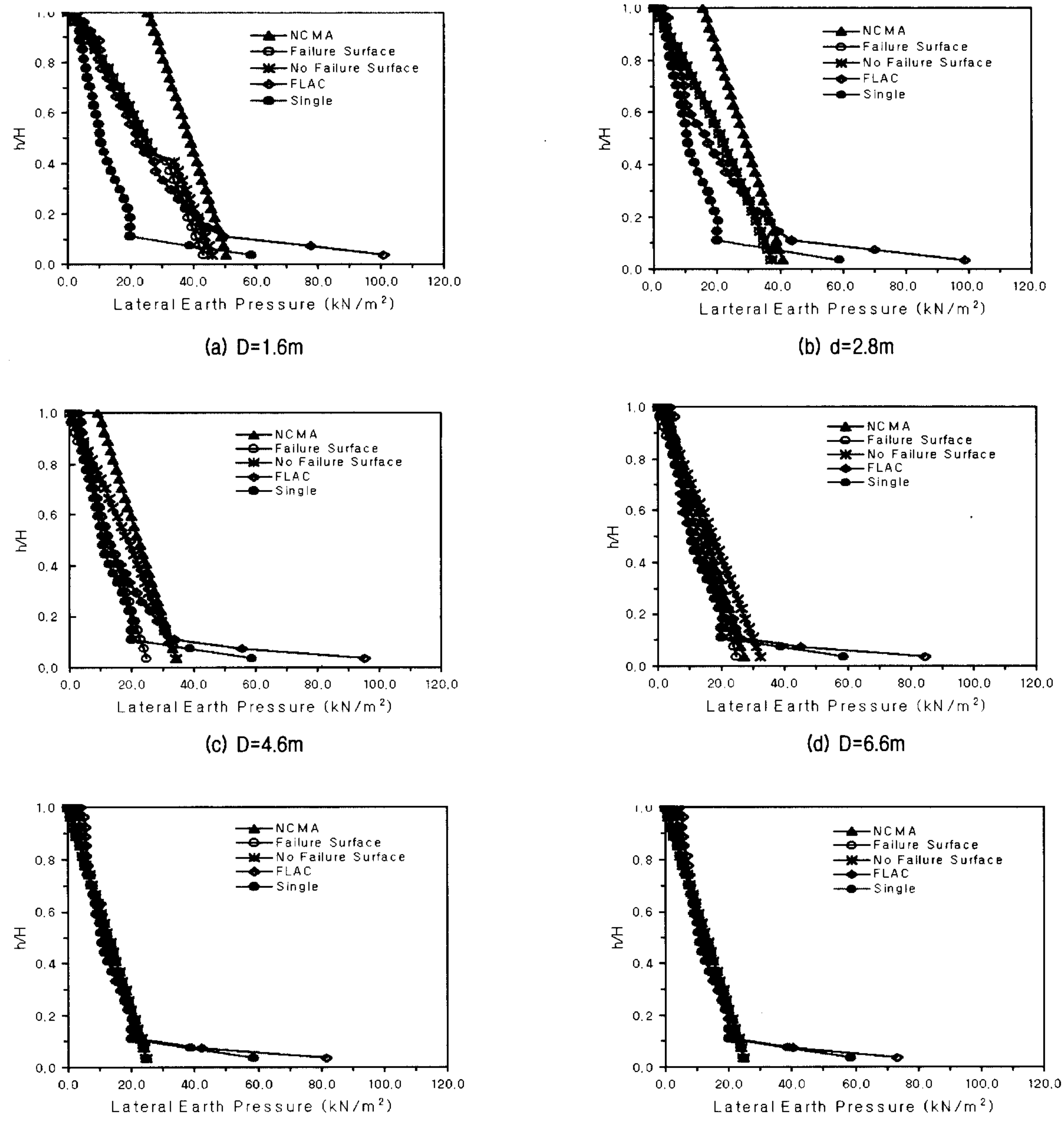

(a) D=1.6m
(b) d=2.8m
(c) D=4.6m
(d) D=6.6m
(e) D=7.6m
(f) D=11.0m

Fig. 16 Comparison of lateral earth pressure behind facing of the lower wall with set back distance D

## 4.2 Lateral Earth Pressure behind Facing

As shown in Fig. 15, the lateral earth pressure behind facing of the upper wall obtained from numerical analysis is generally similar to the Rankine's active earth pressure ($K_a$-line). However, the lateral earth pressure obtained from numerical analysis is greater than $K_a$ and $K_o$ line when the $h/H$ is greater than 0.7. This result seems to be related to the top rotation of upper wall.

Figs. 16(a) through (f) show the comparison of lateral earth pressure behind facing of lower wall obtained from

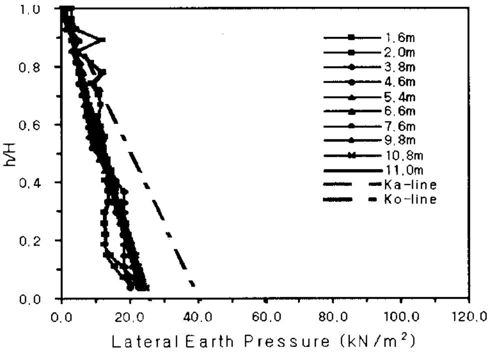


Fig. 17 Lateral earth pressure behind reinforced earth body of the upper wall

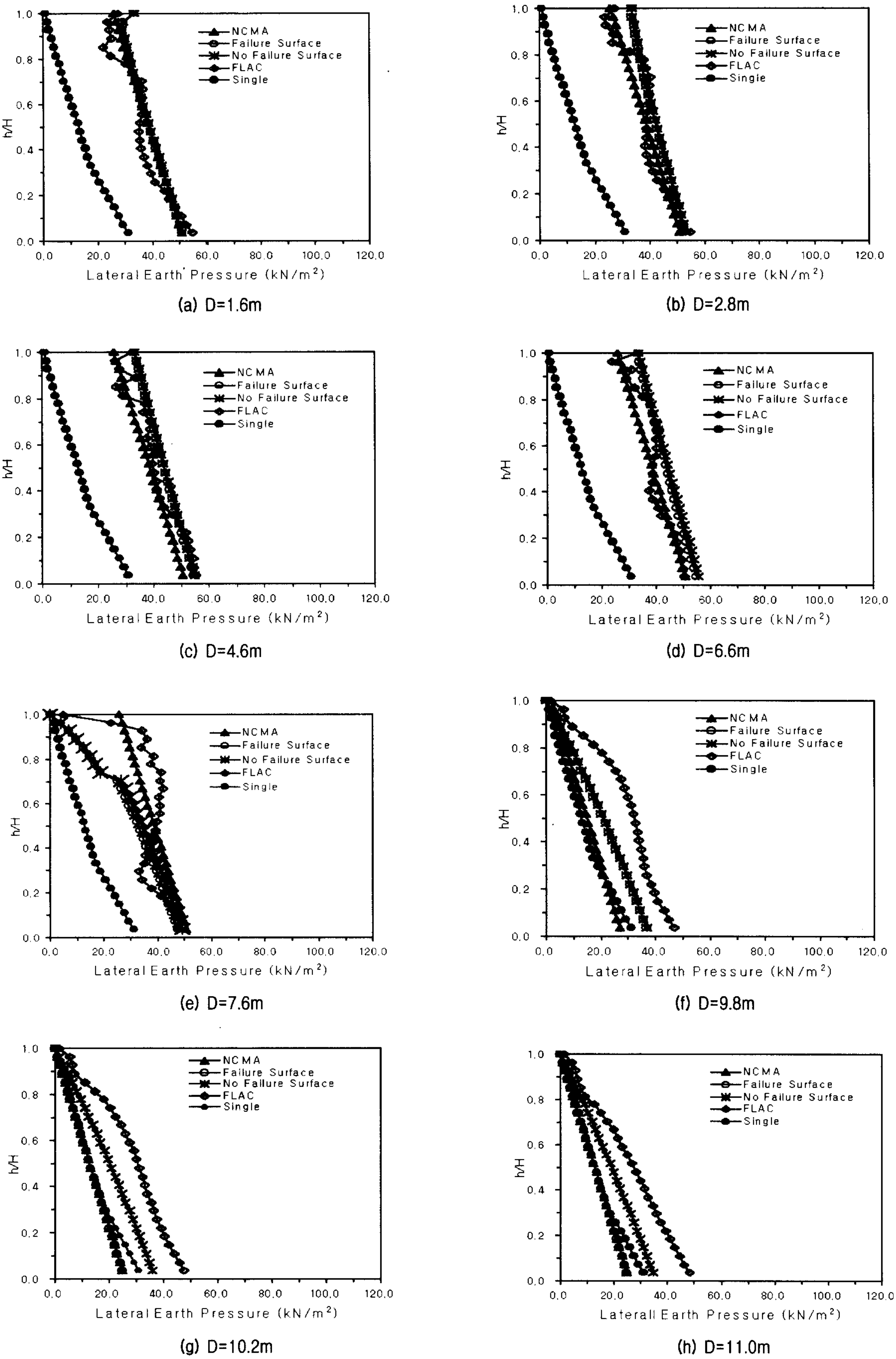


(a) D=1.6m (b) D=2.8m (c) D=4.6m (d) D=6.6m (e) D=7.6m (f) D=9.8m (g) D=10.2m (h) D=11.0m

Fig. 18 Comparison of lateral earth pressure behind reinforced earth body of the lower wall with set back distance D

NCMA method, numerical analysis as well as the 2:1 method considering active failure surface and without considering active failure surface. The result from numerical analysis performed on single wall is presented as well. The results obtained from all the methods tend to decrease with increasing set back distance. As shown in Figs. 16(a) through (c), when the upper wall is located inside the top of the lower reinforced earth body, the calculated lateral earth pressure using NCMA method is greater than those obtained from other methods. This result may be attributed to the application of uniform surcharge on the full area of lower reinforced earth body in NCMA method.

However, the lateral earth pressure obtained from numerical analysis is greater than those from other methods where $h/H$ is under 0.1. This result may be caused by little horizontal displacement due to the friction between facing block and foundation material.

When the set back distance increases as shown in Figs. 16(d) through (f), the distribution of lateral earth pressure obtained from all the methods is similar. Specially, when the upper wall is located on the retained soil of the lower wall, all the result is equal to that of single wall as shown in Figs. 16(e) and (f). Therefore, the lower wall in this case can be treated as independent wall in checking the internal stability.

## 4.3 Lateral Earth Pressure behind Reinforced Earth Body

As shown in Fig. 17, the lateral earth pressure behind reinforced earth body of the upper wall obtained from numerical analysis is generally similar to the Rankine's active earth pressure( $K_a$-line).

Figs. 18(a) through (f) show the comparison of lateral earth pressure behind the reinforced earth body of the lower wall obtained from NCMA method, numerical analysis as well as 2:1 method. These figures also show discrepancy between multi-tiered and single wall. When the upper wall is located inside the top of the lower reinforced earth body, few changes of lateral earth pressure distribution are observed as shown in Figs. 18(a) through (d). When the set back distance increases, as shown in Figs. 18(e) through (h), the predicted lateral earth pressure obtained from numerical analysis is generally greater than those obtained from other methods. Also it is observed that the predicted value from numerical analysis is similar to the value from 2:1 method without considering active failure surface. This result may be caused by decrease of horizontal displacement of lower retained soil body. When the horizontal displacement of lower retained soil due to the self weight of lower reinforced earth body decreases, the lateral earth pressure may be close to $K_o$ condition which is greater than $K_a$ con- dition.

## 4.4 Maximum Tensile Force in the Reinforcement

As shown in Fig. 19, the maximum tensile force in the reinforcement of the upper wall obtained from numerical analysis tend to decrease with increasing set back distance and is constant with large set back distance. Figs. 20(a) through (f) show the comparison of the maximum tensile force in the reinforcement of lower wall obtained from NCMA method, numerical analysis as well as the 2:1 method. The result of numerical analysis performed on single wall is shown as well. The results of all the methods tend to decrease with increasing set back distance.

When $h/H$ is greater than 0.7, the result of numerical analysis is greater than that of 2:1 method as shown in Figs. 20(a) and (b). It may be caused by the self weight

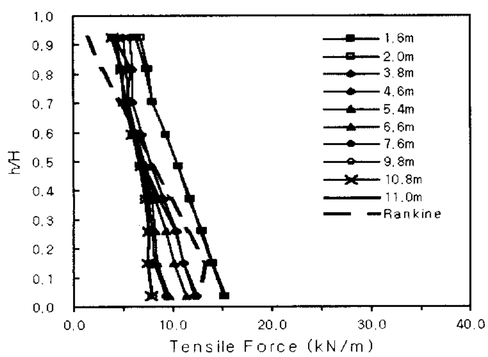


Fig. 19 Maximum tensile force in the reinforcement of the upper wall

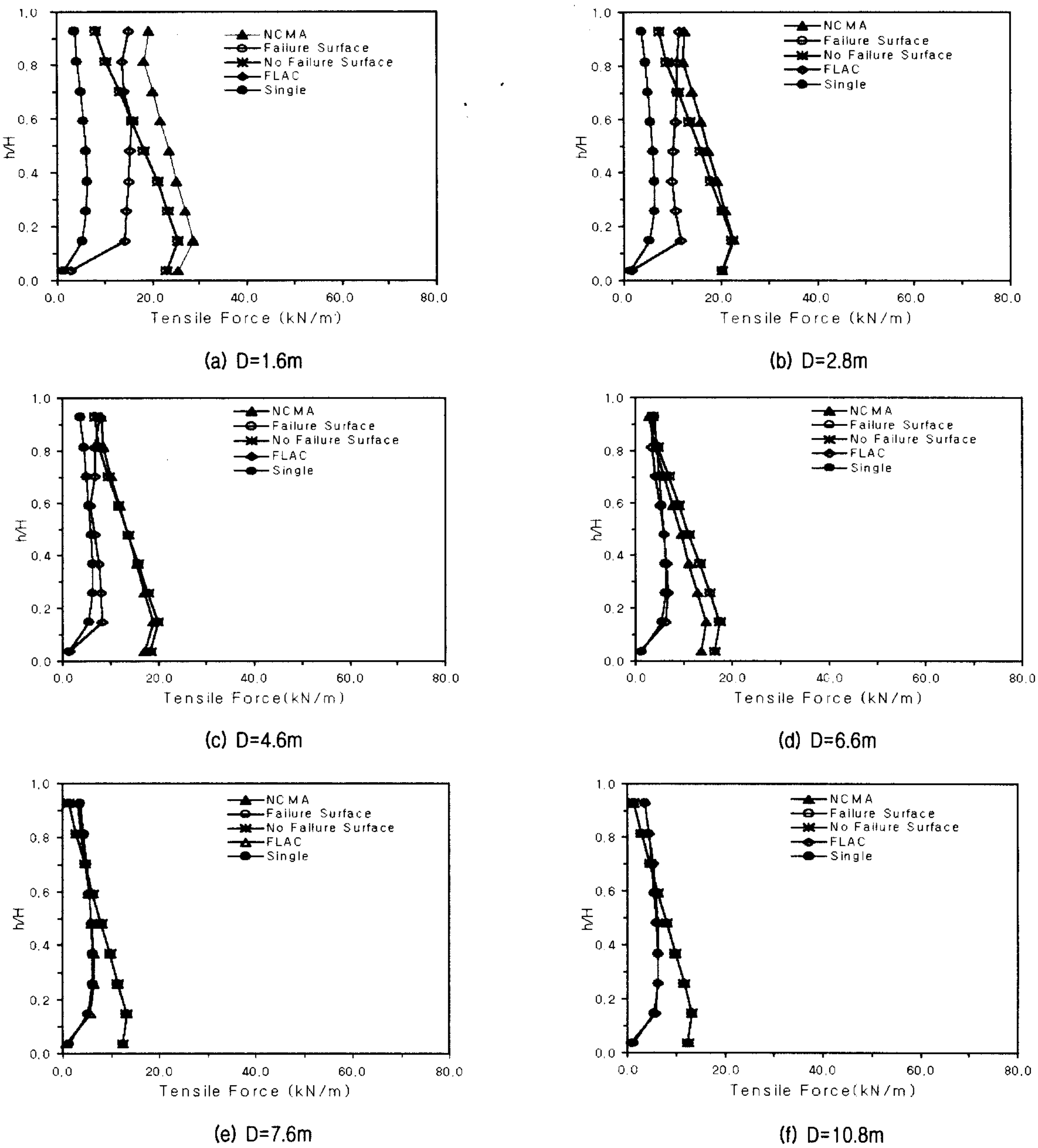


Fig. 20 Comparison of the maximum tensile force in the reinforcement of the lower wall with set back distance D

and Meyerhof stress distribution of the upper wall causing the increase of tensile force in the upper reinforcement. When the upper wall is located on the retained soil of the lower wall as shown in Figs. 20(e) and (f), most results are close to those of the single wall. Therefore, the lower wall in this case can be treated as independent wall in checking the internal stability.

## 5. Conclusion

The theoretical study and numerical analysis were performed in order to assess the behavior of multi-tiered earth retaining wall according to several set back distances. The value obtained from the proposed 2:1 method and NCMA method was compared with the value obtained from numerical analysis. Based on this study, the following conclusion can be drawn.

(1) The horizontal displacement of facing both upper and lower wall obtained from numerical analysis generally decreased with increasing set back distance of upper wall up to 9.8m. When the set back distance was greater than 9.8m, the horizontal displacement of

facing became constant.

(2) The lateral earth pressure behind both facing and reinforced earth body of the upper wall from the numerical analysis was generally similar to the Rankine's active earth pressure.

(3) In the case of lower wall, the lateral earth pressure behind the facing generally decreased with increasing set back distance up to 7.6m whereas the increase or decrease in the lateral earth pressure behind the reinforced earth body was found to depend on the location of upper wall.

(4) The maximum tensile force in the reinforcement of both upper and lower walls gradually decreased with increasing set back distance up to 7.6m.

(5) From the comparison of the lateral earth pressure behind both facing and reinforced earth body, it was observed that the NCMA method was the most conservative and the predicted values from numerical analysis agreed reasonably well with the calculated values obtained from 2:1 method without considering active failure surface.

(6) The critical set-back distance in which the upper wall doses not have influence on the lower can be two times as great as the height of the lower wall.

## References

1. Cundal, P., 1994, FLAC (Fast Lagrangian Analysis of Continua) Version 3.3 Itasca Consulting Group, Inc.
2. Ham, C. H, 1999, "A study on the Behaviour of Reinforced Earth Retaining Wall Considering Condtruction Procedure", M.S. Thesis, Hanyang University.
3. James, K. M and Willem, C. B. V., 1987, *Reinforcement of Earth Slope and Embankments*, Transportation Research Board, Washington, D.C.
4. Jones, C. J. F. P., 1996, *Earth reinforcement and soil structures*, Thomas Telford.
5. Karpurapu, R. and Bathurst, R J., 1995, "Behaviour of geosynthetic reinforced soil retaining walls using the finite element method", *Computers and Geotechnics*, Vol. 17, pp. 279~299.
6. KGS, 1998, Design and construction Manual for Geosynthetics, KGS
7. Kim, H. T, Lee E. S, Song, B. W, 1996, "Evaluation of Tension and Prediction of Deformations for the Fabric Reinforced Earth wall", *Journal of the Korean Geotechnical Socity*, Vol. 12, No. 4, pp. 157~176.
8. Nakane, A., Taki, M., Yokota, Y., and Miyatake, H., 1996, "FEM comparative analysis of facing rigidity of geotextile-reinforced soil walls", *Proc. International Symposium on Earth Reinforcement Practice, Fukuoka, Kyushu, Japan, Ochiai, Yasufuku & Omine Eds., A.A. Balkema, Rotterdam*, pp. 433~438.
9. NCMA, 1997, *Design Manual for Segmental Retaining Wall*, 2nd Ed., NCMA, Virginia.
10. Raj Jalla, 1999, "Design of multiple level retaining walls", *ASCE Journal of Architectural Engineering*, Vol. 5, No. 3, pp. 82~88.
11. Shin, H. G and Yoo, C .S, 1998, "Development of A Design/ Analysis Program for Reinforced Segmental Retaining Walls", Proceedings of 1998 Geosynthetics, pp. 35~45.
12. Technical Committee on Foundation, 1992, *Canadian Foundation Engineering Manual*, 3rd Ed., Canadian Geotechnical Society.
13. Won, G. W., Hull, T., and De Ambrosis, L., 1996, "Performance of a geosynthetic segmental block wall structure to support bridge abutments", *Proc. International Symposium on Earth Reinforcement Practice, Fukuoka, Kyushu, Japan, Ochiai, Yasufuku & Omine Eds., A.A. Balkema, Rotterdam*, pp. 543~548.
14. Yoo, C. S, Lee, K. M and Shin, H.G, 1998, "Behavior of Soil Reinforced Segmental Retaining Walls", *Proceedings ofthe KGS Fall 1999 National Conference*, pp. 319~326.
15. Yoo, C. S and Lee, K. M, 1999, "Behavior of Mechanically Stabilized Earth Retaining Wall with Different Construction Sequence", *Proceedings of the KGS Fall 1999 National Conference*. pp. 473~480.
16. Yoo, C. S, 1999, "Review of Current Design Practice for Soil-Reinforced Segmental Retaining Walls", *Special Seminar on Geosynthetics 2000, Korea*, pp. 41~50.

(received on May 7, 2001)